

Transient crystalline superlattice generated by a photoacoustic transducer

A. Loether,¹ Y. Gao,^{1,2} Z. Chen,¹ M. F. DeCamp,¹ E. M. Dufresne,²
 D. A. Walko,² and H. Wen²

¹*Department of Physics and Astronomy, University of Delaware, Newark, Delaware 19716, USA*

²*Argonne National Laboratory, Argonne, Illinois 60439, USA*

(Received 29 October 2013; accepted 18 February 2014; published online 4 March 2014)

Designing an efficient and simple method for modulating the intensity of x-ray radiation on a picosecond time-scale has the potential to produce ultrafast pulses of hard x-rays. In this work, we generate a tunable transient superlattice, in an otherwise perfect crystal, by photoexciting a metal film on a crystalline substrate. The resulting transient strain has amplitudes approaching 1%, wavevectors greater than 0.002 \AA^{-1} , and lifetimes approaching 1 ns. This method has the potential to generate isolated picosecond x-ray bursts with scattering efficiencies in excess of 10%. © 2014 Author(s). All article content, except where otherwise noted, is licensed under a Creative Commons Attribution 3.0 Unported License.

[<http://dx.doi.org/10.1063/1.4867494>]

Time-resolved x-ray diffraction (TRXRD) has become a very powerful tool for visualizing transient strains in laser excited materials. Utilizing the structural sensitivity of x-ray diffraction with time-resolved pump-probe techniques provides an unique measurement ability to visualize transient structural changes in materials ranging from simple crystals¹⁻⁴ to protein crystals.^{5,6} Currently, one of the challenges of using TRXRD is the ability to either visualize picosecond changes in x-ray intensity and/or producing picosecond isolated bursts of x-ray radiation at hard x-ray synchrotron facilities. Several methods now exist that can produce and/or measure sub-picosecond bursts of x-ray radiation at synchrotron sources.⁷⁻¹² However, these methods often require significant resources (including massive infrastructure improvements) and are often very inefficient. For example, the efficiency of hard x-ray streak cameras are limited by the quantum efficiency of the photo-cathode (typically less than 1%) and the need to limit temporal dispersion by space charge effects.⁸

By modulating the crystalline structure on an ultrafast time-scale, it is possible to isolate a single x-ray pulse from a third generation x-ray source¹³ as well as slice hard x-ray pulses into picosecond bursts.^{14,15} For example, the coherent vibration of an engineered crystalline superlattice can produce high-wavevector coherent acoustic modes that can be stimulated by optical means.¹⁶⁻²⁰ However, as the crystalline superstructure is permanently imbedded into the crystalline sample, it is difficult to completely isolate a picosecond burst of x-ray radiation from the background scattering. In addition, the efficiency of such method is currently limited to $\sim 0.1\%$.²⁰

In this work, we demonstrate the ability to generate a high-fidelity, high-amplitude ultrafast transient superlattice onto an otherwise perfect crystal using a single laser pulse. This transient strain produces localized sidebands on an isolated x-ray Bragg peak, with a diffraction efficiency in excess of 10% and an implied modulation period of less than 20 ps. This method has the potential to modulate a hard x-ray pulse train with near 100% contrast on a picosecond timescale.

Diffraction sidebands on an x-ray Bragg peak reveals the presence of additional wavevectors existing in a crystalline material. In particular, it has been shown that for symmetric x-ray reflections, the wavevector of a particular strain mode (q) in the crystal is given by^{21,22}

$$q = \frac{\Delta\theta|\vec{G}|}{\tan\theta_b}, \quad (1)$$

where \vec{G} is the reciprocal lattice vector of the Bragg peak located at θ_b , and $\Delta\theta$ is the angular deviation from the Bragg condition of the substrate. Coupling one-dimensional x-ray Bragg diffraction with pump-probe techniques has the potential to accurately reconstruct the shape of a localized longitudinal strain pulse.²³ In this work, we demonstrate that under intense optical excitation, a metallic film will generate a periodic strain wave that propagates into the crystalline substrate. The wavevectors of the additional strain components are inversely related to the film thickness and exist within the crystal for over a nanosecond, indicating that the strain is not just a localized pulse but rather a transient periodic strain.

Experiments were performed at the insertion device beamline 7-ID at Advanced Photon Source (APS) at Argonne National Laboratory.²⁴ The sample preparation was described in detail previously²³ and consisted of a series of gold coated samples, with thicknesses of 50, 100, and 270 nm, on a Ge(111) substrate. The measured width of the Au(111) diffraction peak indicates that the film is polycrystalline. Laser excitation was provided by a 50 fs, 400 nm light pulse, 1 kHz laser system synchronized to the APS x-ray train. The laser pulse was focused to a $\sim 1 \text{ mm}^2$ spot on to the sample and the laser intensity was controlled by a half-waveplate/polarizer pair. The laser intensity was kept below the observed damage threshold for the gold films.

Upon 400 nm optical excitation, $\sim 15\%$ of the incident laser energy is absorbed in the near surface, causing a rapid (sub-5 ps) thermal excitation of the gold film.^{23,25} The resulting expansion and relaxation of the gold causes an isolated strain wave to be generated in the crystalline substrate.^{23,26}

To visualize the laser induced strain, the sample was probed by a ~ 100 ps monochromatic x-ray pulse at 8.05 keV. A combination of a focusing Kirkpatrick-Baez mirror pair and x-ray slits resulted in an x-ray spot size of $\sim 100 \times 100 \mu\text{m}^2$ at the crystal surface. The relative time delay between the optical and x-ray pulses was controlled by electronic means with a minimum step size of 19 ps, which is well below the APS x-ray pulse length. TRXRD data were taken in the “top-up” mode, and the measured diffraction curves were the normalized to account for variations in x-ray intensity. The Bragg diffracted x-rays were collected using a gated fast Avalanche Photo Diode (APD) in both proportional and in Geiger counting modes.

The angular shift of the Au(111) peak allowed the calibration of the quasi-instantaneous thermal temperature of the metallic film (see Figure 2(a) inset). Immediately upon optical excitation, rapid generation and decay of ballistic photo excited electrons in the film result in the Au(111) peak shifting by up to 0.2° , indicating that the temperature of the gold film has risen ~ 250 K, implying an incident optical fluence of $\sim 10 \text{ mJ/cm}^2$, consistent with the optical parameters of the laser system and prior published results.^{23,25} At these laser intensities, the gold film did not appear visibly damaged and the Au(111) diffraction peak returned to its pre-excited state in a few nanoseconds.

At the onset of laser excitation, there is a rapid generation of diffraction sidebands on both the compression and rarefaction sides of the Ge(111) diffraction peak (see Figure 1). These sidebands rapidly return to the diffraction peak in a couple hundred of picoseconds, including a coherent modulation of the x-ray intensity, indicating the existence of a localized bipolar longitudinal strain pulse propagating into the substrate.²⁻⁴ As we increase the laser intensity, the sidebands generated by the acoustic disturbance is comparable to the intensity of the main diffraction peak, indicating a substantial strain has been generated into the substrate.

The 270 nm sample has a significantly less intense sideband production, indicating a smaller induced strain, likely due to the significant thermal diffusion within the gold sample.²⁷ After the longitudinal pulse exits the x-ray diffraction region ($\sim 1 \mu\text{m}$), the Ge(111) diffraction peak does not appear to be appreciably shifted, indicating that the substrate has not been heated substantially.

After the longitudinal acoustic pulse has left the diffraction region, there remains two isolated sidebands on either side of the diffraction peak for the 50 and 100 nm samples, at a deviation angle of ~ 15 and ~ 30 mdeg, respectively (see Figure 1). These sidebands are generated within 150 ps and exist for over 1 ns (see Figure 2(b)). The sidebands appear to be located symmetrically on either side of the diffraction peak, with the positive sideband amplitude approximately double the negative sidebands. These two symmetrically placed sidebands suggest the generation of a transient superlattice structure within the crystalline substrate.

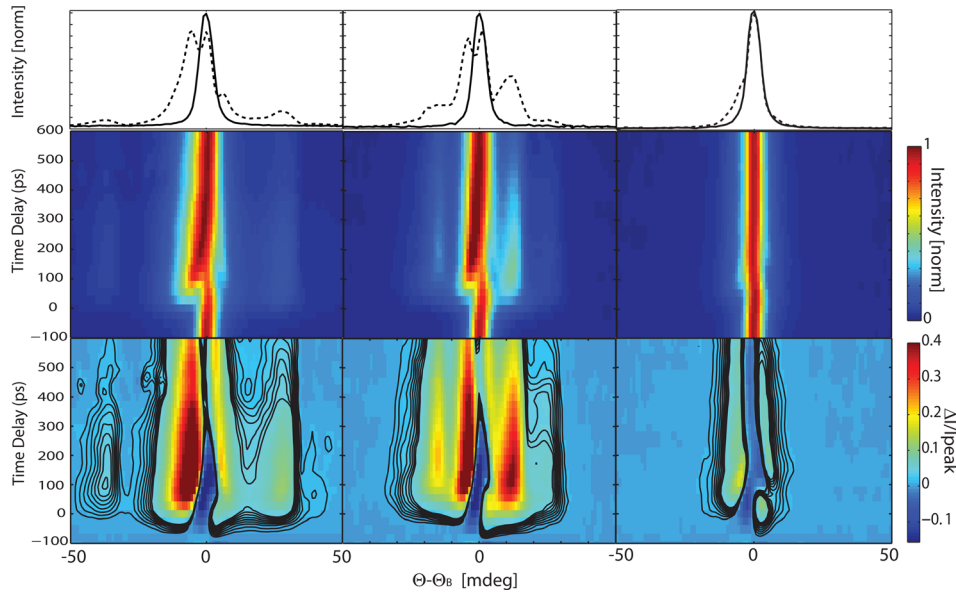


FIG. 1. TRXRD of laser excited 50 nm (left), 100 nm (middle), and 270 nm (right) Au film on a Ge(111) substrate. Top: Diffraction intensities before (solid) and 120 ps (dashed) after laser excitation. Center: TRXRD surfaces of the Ge(111) peak. Bottom: Differential diffraction intensity as a function of time. Contours levels represent changes in x-ray intensity of 0.5% of the main Bragg peak.

Using Eq. (1), the location of the sidebands indicate that the transient superlattice has a periodicity of ~ 150 nm and ~ 300 nm for the 50 nm and 100 nm films, respectively. Given the difference in sound speed between the Ge substrate (5400 m/s) and the Au film (3600 m/s), the observation is consistent with energy from a coherent acoustic vibration within the film, whose period is given by the ratio of the film thickness to the sound velocity, being deposited into the crystalline substrate. If we follow this trend, the 270 nm sample should also possess a superlattice structure of ~ 750 nm. However, given the parameters of the APS x-ray pulse, we are not able to uniquely separate this periodicity from the native Bragg peak of the crystalline substrate and the generated coherent acoustic pulse.

The amplitude of the sidebands is clearly dependent on the optical intensity (Figure 2(a)). In particular, for the 100 nm coated sample, the sidebands have a peak amplitude of $\sim 40\%$ of the main diffraction peak at an optical intensity of $\sim 10 \frac{\text{mJ}}{\text{cm}^2}$. In addition, negative sidebands display a slight dip in diffraction efficiency immediately after laser exposure and rise in diffraction intensity ~ 50 ps after the positive sidebands, consistent with a bipolar strain with the compression layers leading the expansion layer.^{4,23} The sidebands appear to decay in amplitude with a time constant of 450 ± 20 ps for the compression sideband and 580 ± 20 ps for the expansion sideband. This decay time is consistent with a localized superlattice propagating out of the x-ray detection region at the longitudinal sound velocity. This logic is also consistent with the observed data of the 270 nm thick film, where we observe an intensity modulation of 200 ps, which could imply a $\sim 1 \mu\text{m}$ periodic strain wave propagating into the crystal at the sound velocity.

In addition to a first order sideband, on the compression side, we see clear evidence for a second order sideband at approximately twice the deviation angle for both the 50 and 100 nm samples (see Figure 1). The amplitude of the second order sideband is smaller than the first order sideband by approximately an order of magnitude. The existence of this second order sideband may indicate that the transient superlattice is not symmetric about zero strain.

As the x-ray diffraction pattern can be thought of as the Fourier transform of the crystalline lattice, the isolated high-wavevector sidebands on either side of the diffraction peak indicate the presence of a periodic superlattice within the crystal with a spatial period equal to $T = \frac{2\pi}{qv}$, where v is the sound velocity, which suggests that the laser generated strain has several components: a

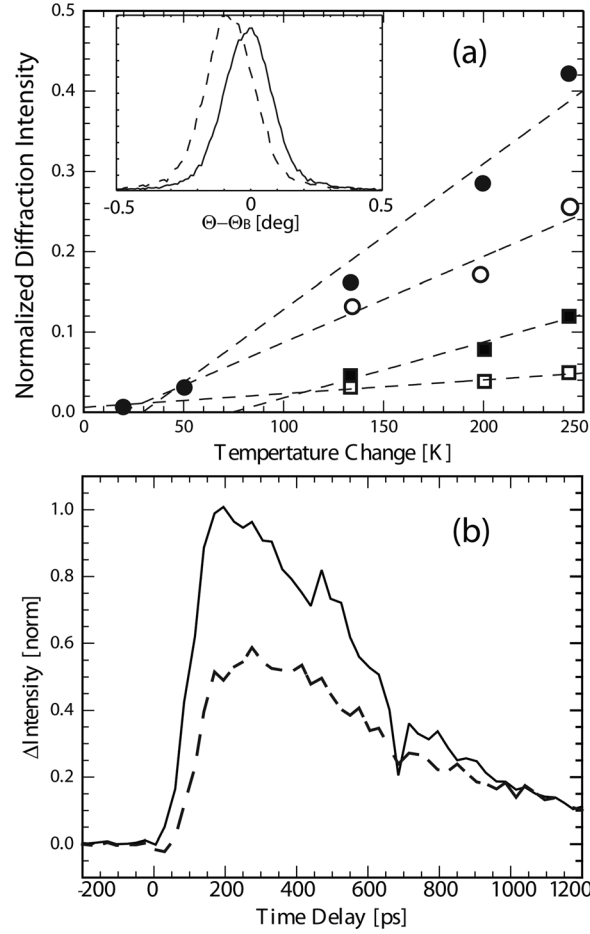


FIG. 2. (a) Induced germanium sideband intensities as a function of inferred lattice temperature. Circles: 100 nm sample. Squares: 50 nm sample. Filled: positive sideband, open: negative sideband. Dashed line is a guide for the eye. Inset: laser induced diffraction shift of the Au(111) diffraction peak. (b) Time-resolved intensity of the positive (solid) and negative (dashed) sidebands of the germanium substrate upon laser excitation for the 100 nm sample.

localized longitudinal acoustic pulse in the sample and a coherent oscillatory component. This oscillatory component likely arises from a coherent acoustic vibration within the gold film which oscillates at a period equal to the ratio of the film thickness to sound velocity.²⁵ Given the high mechanical coupling between the gold film and the crystalline substrate, the coherent vibration will produce a modulated strain wave in the crystalline substrate. In particular, the sound speeds of the gold film and germanium substrate, along with the material densities ($\rho_{Au} \sim 19 \frac{\text{g}}{\text{cm}^3}$, $\rho_{Ge} \sim 5.3 \frac{\text{g}}{\text{cm}^3}$), the predicted reflectivity ($R = \frac{\rho_{Au}v_{Au} - \rho_{Ge}v_{Ge}}{\rho_{Au}v_{Au} + \rho_{Ge}v_{Ge}}$), and transmission ($T = \frac{2\rho_{Au}v_{Au}}{\rho_{Au}v_{Au} + \rho_{Ge}v_{Ge}}$) coefficients for the strain wave at the interface are ~ 0.4 and ~ 1.4 , respectively, which provides a reasonable mechanism for the generation of a substantial strain to be generated into the crystalline substrate.

In order to confirm this model, we compare the experimental data with numerically simulated diffraction curves using the numerical method described by Wie *et al.*²⁸ To replicate the experimental conditions of the APS, we include a convolution to the simulation that results in an effective time-resolution of ~ 50 ps and an x-ray bandwidth of 1.5 eV. The modelled transient strain wave had the following functional form:

$$\eta(t, z) = AX(z') + B \sin\left(\frac{2\pi v_s}{dv_m} z'\right) e^{-z'/\beta}, \quad (2)$$

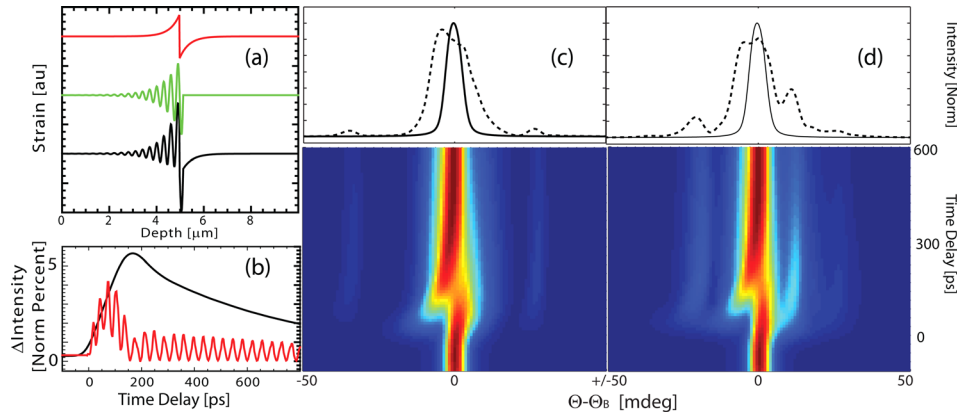


FIG. 3. (a) Simulated strain profile used in the 100 nm simulation at a time delay of ~ 900 ps. Red, single longitudinal pulse; green, transient superlattice; black, full strain wave. (b) Time-resolved x-ray diffraction intensity of the germanium substrate following ultrafast laser excitation of 50 nm gold film sample, at an angular deviation of 30 mdeg from the center of the Bragg peak with (black) and without (red) temporal and angular convolution. (c) TRXRD pattern for laser excited 50 nm sample. (d) TRXRD pattern for a laser excited 100 nm sample. Top: diffraction curves before (solid) and 150 ps (dashed) after laser excitation.

where z' is the retarded position in the crystal given by $z - v_s t$, A and B are the amplitudes of the strain, $X(z')$ is a localized acoustic pulse as described by Thomsen *et al.*,²⁹ β is a characteristic decay of the acoustic vibration (directly related to the reflection coefficient), d is the film thickness, and $v_{s,m}$ is the sound speed in the substrate and metal, respectively (see Figure 3).

Previously, we had shown that the localized acoustic pulse has wavevector components up to the inverse of the film thickness but a spatial extent that approaches $\sim 1 \mu\text{m}$.²³ For this simulation, we assume the pulse has an effective pulse length of 800 nm. When diffraction intensity is simulated using the full strain as given in Eq. (2) and assuming a peak strain of both components of 0.3%, the calculation provides a qualitative agreement to the data (see Figure 3). The effect of the localized acoustic pulse is not visible after ~ 300 ps, the localized high-wavevector sidebands at the correct angles, the decay is on a time-scale consistent with the experimental results, and we can see evidence for the existence of a second order positive sideband.

While the temporal resolution of the APS did not allow us to visualize the temporal modulations within the high-wavevector sidebands, we also investigated the numerical simulation without the temporal convolution (see Figure 3(b)). In particular, after a time delay of 200 ps, the effects of the localized acoustic pulse have been eliminated, leaving a high-frequency coherent modulation in the x-ray intensity that has a scattering amplitude in excess of 1.5% of the native Bragg peak, with near 100% contrast. Experimentally, these high-contrast coherent oscillations could be observed directly with a picosecond x-ray streak camera⁸ and/or a coherent control measurement of the acoustic phonon generation.³⁰

In conclusion, we have demonstrated, for the first time, the generation of a large amplitude transient superlattice in an otherwise perfect crystalline substrate by intense photo excitation of a metallic photo-acoustic transducer. As the frequency of these oscillations are dictated by the film, by reducing the film thickness to the optical absorption depth in the metal (~ 15 nm), we anticipate that high-contrast modulations of the x-ray intensity can be as small as a few picoseconds. These oscillations are likely temporally coherent, allowing the possibility for coherently controlling the picosecond strain using multiple laser pulses,^{30,31} thereby having the potential to generate an efficient picosecond switch for hard x-ray radiation.

This work was supported from the DOE-EPSCoR Grant No. DE-FG02-11ER46816. Use of the Advanced Photon Source was supported by the U.S. Department of Energy, Office of Science, Office of Basic Energy Sciences, under Contract No. DE-AC02-06CH11357.

¹J. Wark, R. Whitlock, A. Hauer, J. Swain, and P. Solone, *Phys. Rev. B* **35**, 9391 (1987).

²C. Rose-Petrucci *et al.*, *Nature* **398**, 310 (1999).

- ³A. Lindenberg *et al.*, *Phys. Rev. Lett.* **84**, 111 (2000).
- ⁴D. A. Reis, M. F. DeCamp, P. H. Bucksbaum, R. Clarke, E. M. Dufresne, M. Hertlein, R. Merlin, R. Falcone, H. Kapteyn, M. Murnane, J. Larsson, T. Missalla, and J. S. Wark, *Phys. Rev. Lett.* **86**, 3072 (2001).
- ⁵F. Schotte, M. Lim, T. Jackson, A. Smirnov, J. Soman, J. Olson, G. Phillips, M. Wulff, and P. Anfinrud, *Science* **300**, 1944 (2003).
- ⁶F. Schotte, H. S. Cho, V. R. I. Kaila, H. Kamikubo, N. Dashdorj, E. R. Henry, T. J. Graber, R. Henning, M. Wulff, G. Hummer, M. Kataoka, and P. A. Anfinrud, *Proc. Natl. Acad. Sci.* **109**, 19256 (2012).
- ⁷R. Schoenlein, S. Chattopadhyay, H. Chong, T. Glover, P. Heimann, C. Shank, A. Zholents, and M. Zolotarev, *Science* **287**, 2237 (2000).
- ⁸Z. Chang, A. Rundquist, J. Zhou, M. Murnane, H. Kapteyn, X. Liu, B. Shan, J. Liu, L. Niu, M. Gong, and X. Zhang, *Appl. Phys. Lett.* **69**, 133 (1996).
- ⁹J. Larsson, Z. Chang, E. Judd, P. Schuck, R. Falcone, P. Heimann, H. Padmore, H. Kapteyn, P. Bucksbaum, M. Murnane, R. Lee, A. Machacek, J. Wark, X. Liu, and B. Shan, *Opt. Lett.* **22**, 1012 (1997).
- ¹⁰A. Zholents, P. Heimann, M. Zolotarev, and J. Byrd, *Nucl. Instrum. Methods Phys. A* **425**, 385 (1999).
- ¹¹A. Cavalieri, D. Fritz, S. Lee, P. Bucksbaum, D. Reis, J. Rudati, D. Mills, P. Fuoss, G. Stephenson, C. Kao, D. Siddons, D. Lowney, A. MacPhee, D. Weinstein, R. Falcone, R. Pahl, J. Als-Nielsen, C. Blome, S. Dusterer, R. Ischebeck, H. Schlarb, H. Schulte-Schrepping, T. Tschentscher, J. Schneider, O. Hignette, F. Sette, K. Sokolowski-Tinten, H. Chapman, R. Lee, T. Hansen, O. Synnnergren, J. Larsson, S. Techert, J. Sheppard, J. Wark, M. Bergh, C. Caleman, G. Huldt, D. van der Spoel, N. Timneanu, J. Hajdu, R. Akre, E. Bong, P. Emma, P. Krejcik, J. Arthur, S. Brennan, K. Gaffney, A. Lindenberg, K. Luening, and J. Hastings, *Phys. Rev. Lett.* **94**, 114801 (2005).
- ¹²W. Leemans, R. Schoenlein, P. Volfbeyn, A. Chin, T. Glover, P. Balling, M. Zolotarev, K. Kim, S. Chattopadhyay, and C. Shank, *Phys. Rev. Lett.* **77**, 4182 (1996).
- ¹³A. Grigoriev, D.-H. Do, D. Kim, C.-B. Eom, P. Evans, B. Adams, and E. Dufresne, *Appl. Phys. Lett.* **89**, 021109 (2006).
- ¹⁴P. Bucksbaum and R. Merlin, *Solid State Commun.* **111**, 535 (1999).
- ¹⁵M. DeCamp, D. Reis, P. Bucksbaum, B. Adams, J. Caraher, R. Clarke, C. Conover, E. Dufresne, R. Merlin, V. Stoica, and J. Wahlstrand, *Nature* **413**, 825 (2001).
- ¹⁶P. Sondhaus, J. Larsson, M. Harbst, G. Naylor, A. Plech, K. Scheidt, O. Synnnergren, M. Wulff, and J. Wark, *Phys. Rev. Lett.* **94**, 125509 (2005).
- ¹⁷M. Bargheer, N. Zhavoronkov, Y. Gritsai, J. Woo, D. Kim, M. Woerner, and T. Elsaesser, *Science* **306**, 5702 (2004).
- ¹⁸M. Trigo, Y. Sheu, D. A. Arms, S. Ghimire, R. Goldman, E. Landahl, R. Merlin, E. Peterson, M. Reason, and D. Reis, *Phys. Rev. Lett.* **101**, 025505 (2008).
- ¹⁹P. Gaal, D. Schick, M. Herzog, A. Bojahr, R. Shayduk, J. Goldshteyn, H. Navirian, W. Leitenberger, I. Vrejoiu, Kh. M. Wulff, and M. Bargheer, *Appl. Phys. Lett.* **101**, 243106 (2012).
- ²⁰M. Herzog, A. Bojahr, J. Goldshteyn, W. Leitenberger, I. Vrejoiu, D. Khakhulin, M. Wulff, R. Shayduk, P. Gaal, and Barg, *Appl. Phys. Lett.* **100**, 094101 (2012).
- ²¹J. Wark, A. Allen, P. Ansbro, P. Bucksbaum, Z. Chang, M. F. DeCamp, R. Falcone, P. Heimann, S. Johnson, I. Kang, H. Kapteyn, J. Larsson, R. Lee, A. Lindenberg, R. Merlin, T. Missalla, G. Naylor, H. Padmore, D. Reis, K. Scheidt, A. Sjoegren, P. Sondhaus, and M. Wulff, *Proc. SPIE* **4143**, 26 (2001).
- ²²J. Larsson, A. Allen, P. Bucksbaum, R. Falcone, A. Lindenberg, G. Naylor, T. Missalla, D. Reis, K. Scheidt, A. Sjoegren, P. Sondhaus, M. Wulff, and J. Wark, *Appl. Phys. A: Mater. Sci. Process.* **75**, 467 (2002).
- ²³Y. Gao, Z. Chen, Z. Bond, A. Loether, L. Howard, S. LeMar, S. White, A. Watts, B. Walker, and M. DeCamp, *Phys. Rev. B* **88**, 014302 (2013).
- ²⁴E. Dufresne, B. Adams, D. Arms, M. Chollet, E. Landahl, Y. Li, D. Walko, and J. Wang, in *Proceedings of the SRI2009, 10th International Conference on Radiation Instrumentation*, edited by K. N. S. W. R. Garrett and I. Gentle (AIP, Melville, NY, 2010).
- ²⁵M. Nicoul, U. Shymanovich, A. Tarasevitch, D. von der Linde, and K. Sokolowski-Tinten, *Appl. Phys. Lett.* **98**, 191902 (2011).
- ²⁶Y. Gao and M. F. DeCamp, *Appl. Phys. Lett.* **100**, 191903 (2012).
- ²⁷S. Brorson, J. Fujimoto, and E. Ippen, *Phys. Rev. Lett.* **59**, 1962 (1987).
- ²⁸C. R. Wie, T. A. Tombrello, and J. T. Vreeland, *J. Appl. Phys.* **59**, 3743 (1986).
- ²⁹C. Thomsen *et al.*, *Phys. Rev. B* **34**, 4129 (1986).
- ³⁰A. Lindenberg, I. Kang, S. Johnson, R. Falcone, P. Heimann, Z. Chang, R. Lee, and J. Wark, *Opt. Lett.* **27**, 869 (2002).
- ³¹N. Del Fatti, C. Voisin, D. Christofilos, F. Vallee, and C. Flytzanis, *J. Phys. Chem. A* **104**, 4321 (2000).